2006

Experimental Study of the Integration of a Scroll Expander Into a Heat Recovery Rankine Cycle

Vincent Lemort
University of Liege

Ion Vladut Teodorese
University of Liege

Jean Lebrun
University of Liege

EXPERIMENTAL STUDY OF THE INTEGRATION OF A SCROLL EXPANDER INTO A HEAT RECOVERY RANKINE CYCLE

Vincent LEMORT[1]*, Ion Vladut TEODORESE[2], Jean LEBRUN[3]

[1,2,3] University of Liège, Thermodynamics Laboratory,
Liège, Belgium
[1,2,3] Phone: +32 4 366 48 24, Fax : +32 4 366 48 12,
[1]vincent.lemort@ulg.ac.be *Author for Correspondence

[2]IonVladut.Teodorese@ulg.ac.be

[3]j.lebrun@ulg.ac.be

ABSTRACT

This study investigates the possibility to associate a scroll expander to a heat recovery Rankine cycle, working with water. In view to develop such a scroll expander, three scroll compressors are adapted to be run in expander mode. The three tested expanders are fed with water steam and air. Two of them need to be lubricated. The third expander is also fed with a binary mixture of water and propylene glycol. A model of scroll expander is proposed and validated.

1. INTRODUCTION

Positive displacement machine can find applications in expander mode. Platell (1993) investigated the potential of screw expanders for the application in small-scale cogeneration, as alternative to turbo expanders. Kane *et al.* (2002) studied the integration of a scroll expander in a Rankine cycle associated to a solar power plant. Xiaojun *et al.* (2004) studied the performances of an air scroll expander used for recovering the energy of exhaust high-pressure air from a proton exchange membrane fuel cell. Huff *et al.* (2002) proposed to use a work-extracting expansion process, instead of the isenthalpic throttling process, in order to improve the CO_2 refrigeration cycle performance. Their simulation study covered piston, scroll, rotary piston, rotary vane and screw expanders. Baek *et al.* (2005) designed, constructed and tested a reciprocating expander, also to replace the expansion valve in an experimental CO_2 transcritical cycle. The study presented here investigates the possibility to associate a scroll expander to a heat recovery Rankine cycle, working with water. The heat source of this cycle could consist in a solar system or in hot gases from an internal combustion engine or a small gas turbine.

2. TESTS ON SCROLL EXPANDERS

In view to develop a scroll expander associated to a heat recovery Rankine cycle, three scroll compressors are adapted to be run in expander mode The three tested expanders are fed with water steam and air. Two of them need to be lubricated. The third expander is also fed with a binary mixture of water and propylene glycol.

2.1 Test bench

The steam test bench comprises two boilers, a super-heater, a pressure stabilization device (release valve), the expander itself and a condenser. Moreover, the shaft of the expander drives an asynchronous machine through a belt-and-pulley coupling. The asynchronous machine imposes the rotational speed of the expander, which can be

adapted by varying the pulley ratio. The air test bench comprises the same components, except an air compressor replaces the boiler.

Temperatures and pressures are measured upstream and downstream from the expander. The mechanical power of the expander is determined by measuring simultaneously the rotational speed and the torque developed at the expander shaft. The electrical power delivered by the asynchronous generator is also measured. After calibration of the generator, this electrical power gives a second measurement of the mechanical power delivered by the expander.

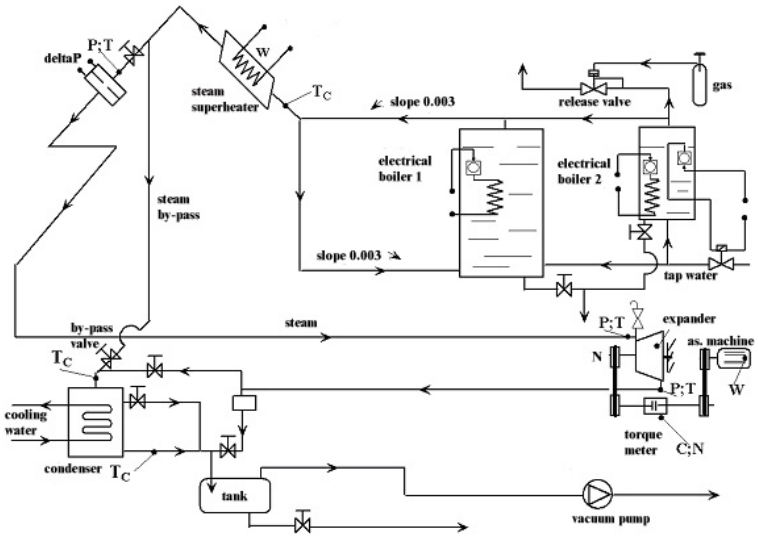

Figure 1: Schematic representation of the test bench (with water as working fluid)

2.2 Description of the expanders

The first expander (expander *A*) is originally an oil-free open-drive air scroll compressor. The back side of the two scrolls is covered by fins to ensure good cooling down of the compressor. A particularity of this scroll compressor is the presence of a moving seal embedded in a groove at the tip of each scroll. The internal surface of each seal is in contact with the high-pressure region of the compressor. Under action of the high pressure, each seal rises and closes the gap between the base of one scroll and the tip of the other scroll, decreasing axial leakage.

The second expander (expander *B*) is originally designed for refrigeration application (R404-a). The design of this scroll compressor allows the fixed scroll to have a small degree of axial and radial movement. Axial compliance allows the scroll to remain in continuous contact in all normal operating conditions, ensuring minimal leakage without the use of tip seals. Radial compliance allows the scroll members to separate sideways so debris can pass through, substantially improving durability. Continuous flank contact, maintained by centrifugal force, also minimizes gas leakage.

The third tested machine (expander *C*) is originally designed for automotive air-conditioning (R134-a). It is the smallest of the three tested compressors. Similarly to compressor *A*, one tip seal is nestled in the tip of one of the two scrolls. This tip seal lefts under the action of the high pressure acting on its lower face, which allows leakages to be reduced, while limiting wearing of the two scrolls.

According to the manufacturer, the three compressors present swept volumes of respectively 148, 98 and 60 cm3, and internal built-in volume ratios close to respectively 4.1, 3.1 and 2.6.

2.3 Tests

This study aims at designing a scroll expander associated to a Rankine cycle, characterized by an evaporating pressure ranging from 4 to 9 bar (water saturation temperature comprised between 144°C and 175°C) and a

condensing pressure ranging from 0.5 to 1 bar. Steam superheating degree at the expander supply doesn't exceed 50 K. Expander rotational speeds are limited by the maximal rotational speed allowed in compressor mode, according to manufacturer specifications.

Expander A is first tested with steam and then with air. The thirty-four tests with steam are characterized by different rotational speeds (1500, 2200 and 3500 rpm), supply pressures (5, 6.5 and 8 bar), supply superheating degrees (10 and 50 K) and exhaust pressures (0.5 and 1 bar). Six tests with air are carried out at a rotational speed of 4300 rpm. Figure 2 shows the evolution of the measured global isentropic effectiveness defined in equation (1), with the pressure ratio imposed to the expander (ratio between supply and exhaust pressures) and the evolution of the mechanical power delivered by the expander with the specific volume of the fluid at the expander supply. In some tests, the effectiveness goes beyond 50%.

$$\varepsilon_{s,meas} = \frac{\dot{W}_{sh,meas}}{\dot{M}_{meas}.(h_{su,\exp} - h_{ex,\exp s})} \tag{1}$$

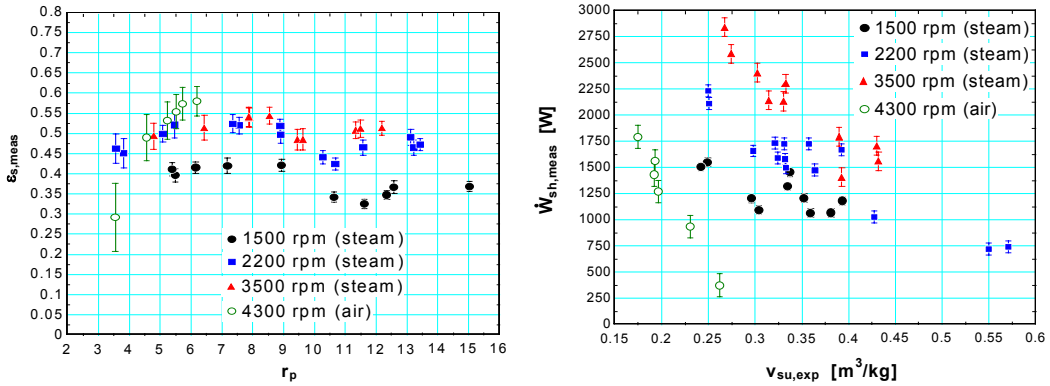

Figure 2: (a) Evolution of the measured isentropic effectiveness with the pressure ratio, (b) Evolution of the delivered mechanical power with the fluid specific volume at the expander supply (expander *A*)

Expander *B* is first tested with air and then with water steam. For all the tests, the expander exhaust pressure is the atmospheric pressure. The supply pressure doesn't exceed 7.5 bar. Consequently, the pressure ratios are quite low. Figure 3 shows that measured isentropic effectiveness is higher with air than with water steam.

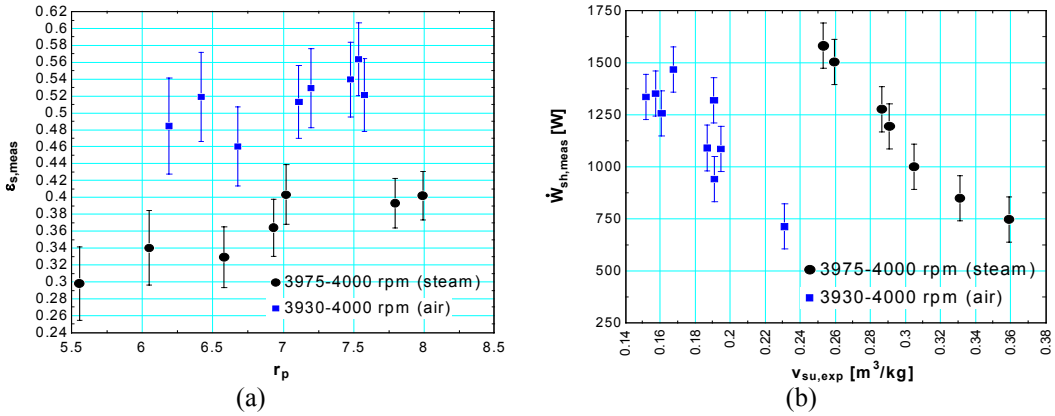

Figure 3: (a) Evolution of the measured isentropic effectiveness with the pressure ratio, (b) Evolution of the delivered mechanical power with the fluid specific volume at the expander supply (expander *B*)

Expander *C* is successively fed with air and propylene glycol, water and lubricating oil and finally water and propylene glycol. Oil and propylene glycol are injected in the air or steam very upstream from the expander supply. For security reasons, the rotational speed of the expander is limited to 3200 rpm. During the five tests with air, suction pressure is not higher than 6.5 bar and discharging pressure is equal to atmospheric pressure. The highest pressure ratio achieved is thus 6.5. With air instead of water, the pressure ratios imposed during these tests lead to volume expansion ratios largely lower than the ones expected with steam in nominal conditions. These low volume expansion ratios are suitable for this machine: in spite of the low level of mechanical power, measured isentropic effectiveness is quite satisfactory: between 0.5 and 0.7.

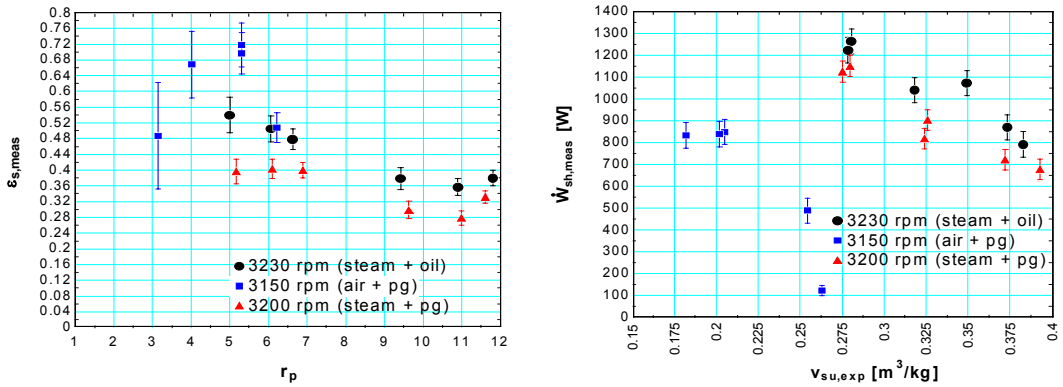

(a) (b)

Figure 4: (a) Evolution of the measured isentropic effectiveness with the pressure ratio, (b) Evolution of the delivered mechanical power with the fluid specific volume at the expander supply (expander *C*)

Six tests are carried out with steam and lubricating oil. These tests are carried out at low rotational speeds (3150 rpm), with suction pressure between 3 and 7 bar and two different discharging pressures: 0.55 and 1 bar. The trend observed with compressed air is confirmed here: the performances of the machine are better at low pressure ratios. For pressure ratios close to 5 or 6, isentropic effectiveness reaches 0.5. When pressure ratio rises up to 10, isentropic effectiveness drops to a value between 0.3 and 0.4. This trend can be seen in Figure 4. The expander is also tested with a binary mixture of propylene glycol and water. Actually, this mixture seems interesting since it may combine lubricating and anti-freezing properties. The mass fraction of propylene glycol is close to 20%. A series of nine tests is achieved at low rotational speed (for preventing any risk of accident) with an important proportion (40 to 60 %) of propylene glycol in the liquid phase and a very important proportion (30 to 40%) of liquid phase at the expander supply (to ensure lubrication). Figure 4 shows the same trend as the one that can be observed with water and oil: isentropic effectiveness decreases when the pressure ratio imposed to the machine is increased. Isentropic effectiveness is lower when using propylene glycol instead of oil, which can be due to a less good lubrication with propylene glycol.

3. SCROLL EXPANDER MODEL

3.1 Description of the expander model

A model of scroll expander is proposed. It is similar to the one developed by Winandy and Lebrun (2002) for hermetic scroll compressors. The evolution of the fluid state through the expander is decomposed into the following steps: cooling-down (su → su,1), isentropic expansion (su,1 → ad), expansion at a fixed volume (ad → ex,2), mixing between suction flow and leakage flow (ex,2 → ex,1) and cooling-down or heating-up (ex,1 → ex). The conceptual scheme of the expander model is shown in Figure 5.

As shown in equation (2), the internal mass flow rate $\dot{M}_{in}$ is the difference between the mass flow rate $\dot{M}$ entering the expander and the leakage mass flow rate $\dot{M}_{leak}$. The entering mass flow rate is the volume flow rate $\dot{V}_{s,\exp}$ divided by the specific volume of the fluid $v_{su,1}$ after entering cooling down. The volume flow rate is the swept volume $V_{s,\exp}$ multiplied by the expander rotational speed N_{rot}. The swept volume in expander mode is equal to the one in compression mode $V_{s,cp}$ divided by the internal built-in volume ratio of the machine r_v.

$$\dot{M}_{in} = \dot{M} - \dot{M}_{leak} = \frac{\dot{V}_{s,\exp}}{v_{su,1}} - \dot{M}_{leak} = \frac{N_{rot}.V_{s,\exp}}{v_{su,1}} - \dot{M}_{leak} = \frac{N_{rot}}{v_{su,1}}.\frac{V_{s,cp}}{r_v} - \dot{M}_{leak} \tag{2}$$

The leakage flow rate can be computed by reference to the flow through a simply convergent nozzle. The fictitious leakage area A_{leak} is assimilated to the nozzle throat and is a parameter of the model to identify.

The internal expansion power $\dot{W}_{in}$ is obtained by multiplying the internal work w_{in} by the internal flow rate. This internal work is the sum of the internal work $w_{in,s}$ associated to the isentropic part of the expansion and internal work $w_{in,v}$ associated to the isochoric evolution. In equation (3), h_{ad}, v_{ad} and P_{ad} are respectively the enthalpy, the specific volume and the pressure of the fluid at the end of the isentropic part of the expansion. The specific volume is the product of the internal built-in volume ratio r_v and the specific volume $v_{su,1}$.

$$\begin{aligned} \dot{W}_{in} &= \dot{M}_{in}.w_{in} = \dot{M}_{in}.\left(w_{in,s} + w_{in,v}\right) = \dot{M}_{in}.\left(\left(h_{su,1} - h_{ad}\right) + v_{ad}.\left(P_{ad} - P_{ex}\right)\right) \\ &= \dot{M}_{in}.\left(\left(h_{su,1} - h_{ad}\right) + r_v.v_{su,1}.\left(P_{ad} - P_{ex}\right)\right) \end{aligned} \tag{3}$$

The expander mechanical power can be split into: the internal expansion power, the constant mechanical losses $\dot{W}_{loss,0}$ and the mechanical losses proportional to the internal expansion power $\alpha.\dot{W}_{in}$. The constant electro-mechanical losses can be expressed as a function of a mechanical losses torque T_m and the rotational speed of the expander. The expander mechanical power is given in equation (4).

$$\dot{W}_{sh} = \dot{W}_{in} - \dot{W}_{loss,0} - \alpha.\dot{W}_{in} = \left(1-\alpha\right).\dot{W}_{in} - \dot{W}_{loss,0} = \left(1-\alpha\right).\dot{W}_{in} - 2.\pi.N_{rot}.T_m \tag{4}$$

A fictitious envelope of uniform temperature T_w is assumed to be able to represent the three heat transfer modes. Steady state balance for this envelope is given in equation (5).

$$\dot{W}_{loss} - \dot{Q}_{ex} - \dot{Q}_{su} - \dot{Q}_{amb} = 0 \tag{5}$$

The fictitious suction heat exchanger of constant wall temperature T_w is modeled by equation (6). The same set of equations is used for the discharge heat transfer. The ambient losses are computed in equation (7), on the basis of a global heat transfer coefficient AU_{amb} (between wall temperature and ambiance temperature).

$$\dot{Q}_{su} = \dot{M}.c_p.(T_{su,1} - T_{su}) = \varepsilon_{su}.\dot{M}.c_p.(T_w - T_{su}) = \left(1 - e^{\left(\frac{-AU_{su}}{\dot{M}.c_p}\right)}\right).\dot{M}.c_p.(T_w - T_{su}) \tag{6}$$

$$\dot{Q}_{amb} = AU_{amb}.(T_w - T_{amb}) \tag{7}$$

3.2 Validation of the model

Parameters of the scroll expander model are identified on basis of tests with steam and air. The simulation flow chart is represented in Figure 3. The supply and exhaust pressures, the supply temperature and the rotational speed are the

inputs of the model. Parameters are tuned in order to get equality between calculated and measured values of the flow rate and the mechanical power. The identified parameters for the three expanders are given in Table 1.

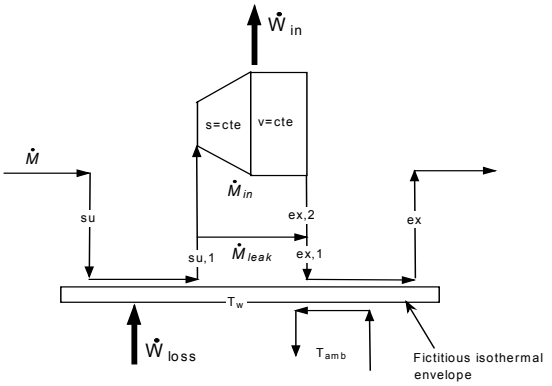

Figure 5: Conceptual scheme of the expander model

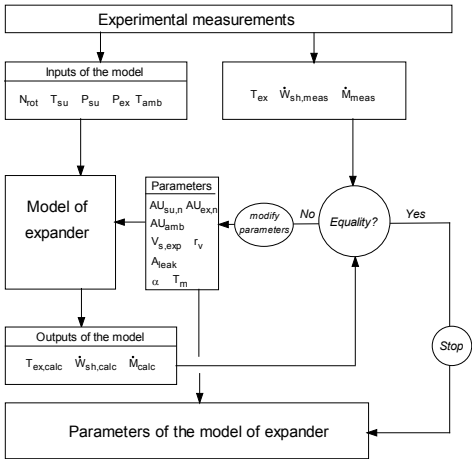

Figure 6: Flow chart for the parameters identification of the expander model

Figure 7 to 9 compare the calculated and measured values of the flow rate and the mechanical power for the three expanders.

Some difficulties are encountered for the identification of the leakage area for test with steam on expander *A*. In Figure 7, the steam flow rate is calculated on basis of a leakage area of 5.0 10^{-6} m^2, but this leakage area seems to vary from one test to another (from 3.0 10^{-6} to 8.5 10^{-6} m^2). The seals may partly or even not rise. The reason might be contact force due to the presence of liquid water under the seals, or fouling of the groove (by calcium carbonate and other particles) where the seals are embedded. In the case of tests with air, the adjustment of parameters is quite good. The identified leakage area is smaller than the one identified for the expander fed with steam.

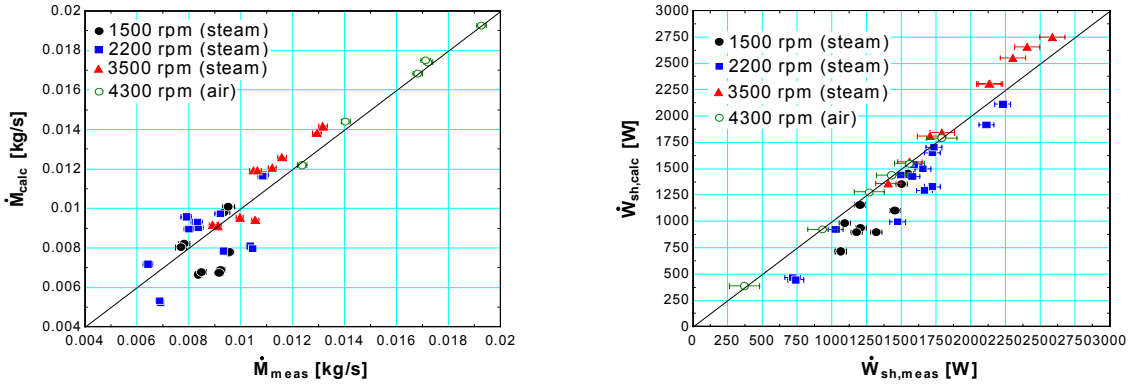

(a) (b)

Figure 7: Prediction of flow rate (a) and mechanical power (b) (expander *A*)

For tests with air on expander *B*, the identified leakage area is 0.5 10^{-6} m^2 (except for the last test in which it is identified to 1.1 m^2, following a probable degradation of the machine). In Figure 8, steam flow rate is calculated on the basis of a leakage area equal to 1.1 10^{-6} m^2. The model adjusted on tests with air seems to underestimate steam flow rate. For tests with water, a losses torque of 2.5 N.m is considered and the proportionality factor α is set to *0*. The model well predicts the mechanical power. Expander *B* reveals a higher mechanical losses torque than expander

A, but a lower leakage area. This can be explained by the tip and base contact, due to axial compliance, which is characteristic of expander *B*.

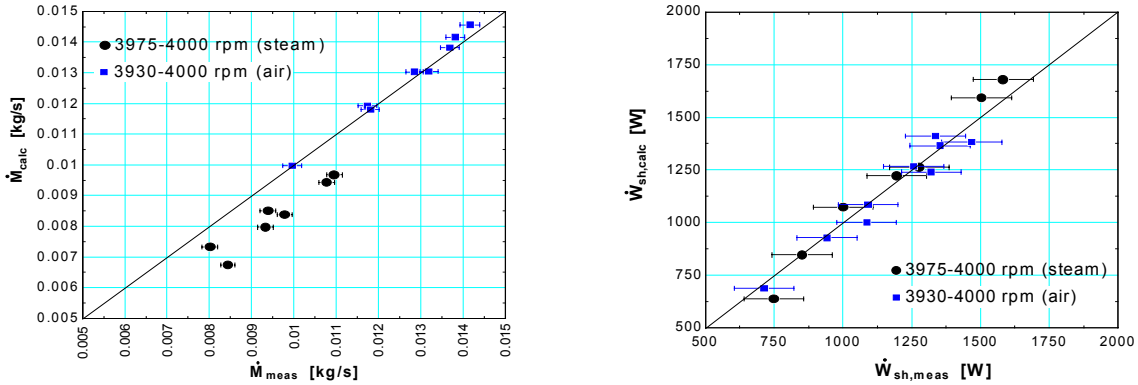

(a) (b)

Figure 8: Prediction of flow rate (a) and mechanical power (b) (expander *B*)

For tests on expander *C*, only a very high leakage area could explain the high air flow rate measured. The tip seal embedded in one of the two scrolls may not lift, leading to an important axial leakage. The leakage area identified on the basis of tests with steam is higher than the one identified on the basis of tests with air. The behavior of the tip seal may not be the same with air than with steam. In Figure 9, for tests with steam and propylene glycol, the mass flow rate is the flow rate of the mixture.

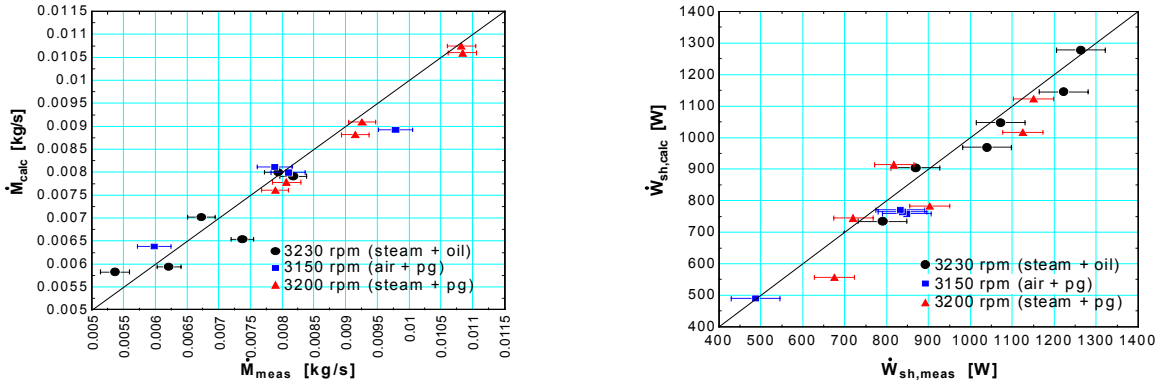

Figure 9: Prediction of flow rate (a) and mechanical power (b) (expander *C*)

Table 1: Synthesis of the identified parameters for the three expanders

exp	*Fluid*	α	T_m [N.m]	$V_{s,cp}$ [cm^3]	$V_{s,exp}$ [cm^3]	r_v	A_{leak} [cm^2]	$AU_{su,n}$ [W/K]	$AU_{ex,n}$ [W/K]	AU_{amb} [W/K]
A	Water	0	0.5	/	38	4.1	3.0- 10^{-6} – 8.5 10^{-6}	6	9	9
A	Air	0.1	1	/	38	4.1	2.0 10^{-6}	6	9	9
B	Air	0.15	1.43	/	31	3.12	0.5 10^{-6} – 1.1 10^{-6}	4	6	7
B	Water	0	2.5	/	31	3.12	1.1 10^{-6}	4	6	7
C	Air + PG	0	0.1	/	23	2.6	2.0 10^{-6}	2	4	5
C	Water + oil	0	0.1	/	23	2.6	4.0 10^{-6}	2	4	5
C	Water + PG	0	0.5	/	23	2.6	4.55 10^{-6}	2	4	5

6. CONCLUSIONS

With water steam as working fluid, expander *A* presents the best isentropic effectiveness (55%) among the three expanders. This effectiveness could be even higher if internal leakage was reduced. This internal leakage is probably due to problems encountered with the seals embedded in the tips of the scroll. Expander *A* is the best adapted to the imposed pressure ratios, since it presents the highest internal built-in volume ratio (4.1). Expander *C* has a too small internal built-in volume ratio (2.6) for the considered application. Friction is the most important in the case of expander *B*. Tests on expander *C* with water and oil and water and propylene glycol show that the latter is not as good as a lubricant than oil. The highest delivered mechanical powers are achieved by expander A (around 3000 W). The model is able to predict the mass flow rate and the mechanical power delivered by the machine. The presence of tip seals makes the leakage area identification more difficult.

NOMENCLATURE

A	area	(m^2)	**Subscripts**	
AU	heat exchange coefficient	(W/K)	ad	adapted
$\dot{M}$	mass flow rate	(kg/s)	amb	ambient
N	rotational speed	(Hz)	calc	calculated
P	pressure	(Pa)	cp	compressor
$\dot{Q}$	heat flux	(W)	ex	exhaust
r_v	volume ratio	(-)	exp	expander
T	temperature	(°C)	in	internal
T	torque	(N.m)	leak	leakage
V_s	swept volume	(m^3)	m	mechanical
v	specific volume	(m^3/kg)	meas	measured
$\dot{V}$	volume flow rate	(m^3/s)	n	nominal
$\dot{W}$	Power	(W)	s	isentropic
			sh	shaft
			su	supply

REFERENCES

Baek, J.S. Groll, E.A., Lawless, P.B., 2005, Piston-cylinder work producing device in a transcritical carbon dioxide cycle. Part I: experimental investigation, *Int. J. Refrig.*, vol. 28 : p.152-164

Huff, H.J., Lindsay, D., Radermacher, R., 2002, Positive displacement compressor and expander simulation, *International Compressor Engineering Conference at Purdue 2002*

Kane, El H. M., 2002, Intégration et optimisation thermoéconomique & environomique de centrales thermiques solaires hybrides, *PhD Thesis, Laboratoire d'Energétique Industrielle, Ecole polytechnique Fédérale de Lausanne, Suisse*

Platell, P., 1993, Displacement expanders for small scale cogeneration, *Licentiate Thesis, Department of Machine Design, Royal Institute of Technology, Stockholm*

Winandy, E.L., Lebrun, J., 2002, Scroll compressors using gas and liquid injection: experimental analysis and modeling, *International Journal of Refrigeration*, vol. 25: p. 1143-1156

Xiaojun, G., Liansheng, L., Yuanyang, Z., Pengcheng, S., 2004, Research on a Scroll Expander Used for Recovering Work in a Fuel Cell, *Int. J. Thermodynamics*, vol. 7: p. 1-8